OPEN ACCESS
JOURNAL OF ADVANCED DIELECTRICS
Vol. 12, No. 1 (2022) 2160011 (7 pages)

DOI: 10.1142/S2010135X21600110

Chemical ordering and magnetic phase transitions in multiferroic $BiFeO_3$–$AFe_{1/2}Sb_{1/2}O_3$ (A-Pb, Sr) solid solutions fabricated by a high-pressure synthesis

S. I. Raevskaya*, N. M. Olekhnovich†, A. V. Pushkarev†, Y. V. Radyush†, S. P. Kubrin*, V. V. Titov*, E. A. Artseva*, I. P. Raevski*,§, I. N. Zakharchenko*, C-C. Chou‡ and M. A. Malitskaya*

*Research Institute of Physics and Faculty of Physics
Southern Federal University
Rostov-on-Don 344090, Russia

†Scientific-Practical Materials Research Centre of NAS of Belarus
220072, Minsk, Belarus

‡ Taiwan University of Science and Technology
Taipei 106, China

§igorraevsky@gmail.com

Received 14 April 2021; Accepted 10 June 2021; Published 16 July 2021

Ceramic samples of $BiFeO_3$-based perovskite solid solutions with the highly ordered complex perovskites $PbFe_{1/2}Sb_{1/2}O_3$ (PFS) and $SrFe_{1/2}Sb_{1/2}O_3$ (SFS) were obtained using high-pressure synthesis at 4–6 GPa. Mössbauer studies revealed that $BiFeO_3$-SFS compositions are characterized by a larger compositional inhomogeneity as compared to $BiFeO_3$-PFS ones. In line with this result, concentration dependence of the magnetic phase transition temperature T_N for $BiFeO_3$-SFS compositions is close to the $T_N(x)$ dependence for $BiFeO_3$ solid solution with disordered perovskite $PbFe_{1/2}Nb_{1/2}O_3$ (PFN). In contrast to this $T_N(x)$ dependence for $BiFeO_3$-PFS compositions nicely follows the theoretical $T_N(x)$ dependence calculated for the case of the ordered distribution of Fe^{3+} and non-magnetic Sb^{5+} ions in the lattice (chemical ordering).

Keywords: Multiferroics; chemical ordering; magnetic phase transition; $BiFeO_3$; high-pressure synthesis.

1. Introduction

$BiFeO_3$ is nowadays, one of the most widely studied material as it exhibits both magnetic and ferroelectric properties at room temperature and well above it.[1] Such materials are called multiferroics and are prospective for a lot of applications.[1–7] For many of these applications, it is necessary to adjust the temperatures of both magnetic and ferroelectric phase transitions to a certain temperature range as the magnetoelectric response increases dramatically in the vicinity of phase transitions.[4,8,9] This problem may be solved e.g., by designing of various solid solutions based on $BiFeO_3$.[1] Formation of solid solutions also gives one a possibility to destroy the spatially modulated spin cycloid being one of the origins of the antiferromagnetic spin ordering in $BiFeO_3$ and limiting its application.[1] Unfortunately, the synthesis of many $BiFeO_3$-based solid solutions with perovskite structure at atmospheric pressure is often limited leading to the necessity of using the high-pressure synthesis.[6,10]

To create new multiferroic solid solutions, it is highly desirable to predict the magnetic phase transition temperature T_N dependence on composition. It is usually considered that in Fe-containing perovskite multiferroics such as $BiFeO_3$ and $PbFe_{1/2}B^{5+}{}_{1/2}O_3$ (B^{5+} – Sb, Nb, Ta,) ferroelectric and magnetic subsystems are independent. The explanation was that ferroelectric properties are provided by bismuth or lead ions located in the A sites of the ABO3 perovskite unit cell, whereas magnetic properties are caused by iron ions located in the B-sites. The A-sublattice appears to be ferroelectrically active due to the dangling bonds or lone electron pairs (nonfilled 6p states) typical of both bismuth and lead ions producing the local electric dipoles.[2,3] Therefore, it is commonly believed that the T_N value in Fe-containing perovskites depends only on the number of possible Fe–O–Fe connections in the lattice, i.e., the amount of the magnetic nearest neighbors at each Fe^{3+} ion.[11] However, recently it was shown that T_N decreased considerably and the long-range antiferromagnetic order transformed into a short-range

§Corresponding author.

spin-glass one as a result of the introduction of nonmagnetic ions into Pb sublattice of $PbFe_{1/2}Nb_{1/2}O_3$ (PFN), although the iron concentration in the B-sublattice remained the same.[12] It was assumed that both classical magnetic superexchange via the Fe–O–Fe bonds and a nontrivial one via the empty 6p states of Pb^{2+} ions coexist in PFN and similar compounds. Subsequently, the X-ray fluorescence holography studies of $PbFe_{1/2}Nb_{1/2}O_3$ proved the participation of Pb ions in the superexchange interaction among Fe ions.[13] A feasibility of a consimilar nontrivial magnetic super exchange among Fe^{3+} ions in $BiFeO_3$ through the empty 6p states of Bi^{3+} was assumed earlier by de Sousa *et al*.[14] Nevertheless, such mechanism of super exchange most likely begins to make a noticeable contribution to the overall super exhange at a rather high concentration of nonmagnetic ions in the Fe-sublattice of $BiFeO_3$-based solid solutions.[15]

It should be stressed that in multiferroic solid solutions as well as in complex Fe-containing multiferroics $PbFe_{1/2}B^{5+}{}_{1/2}O_3$ (B^{5+} –Nb, Ta, Sb) there exists the possibility of notable changing the degree of chemical or compositional ordering of B-cations, well known for other $PbB^{3+}{}_{1/2}B^{5+}{}_{1/2}O_3$ (B^{3+} –In, Sc, Yb, Lu; B^{5+} –Nb, Ta, Sb) perovskites.[16–21] The values of T_N should depend significantly on such ordering as it changes the number of magnetic nearest neighbors at Fe^{3+} ions. Nevertheless, while examining X-ray and neutron diffraction data for the complex Fe-containing perovskite multiferroics $PbFe_{1/2}B^{5+}{}_{1/2}O_3$ (B^{5+} –Nb, Ta, Sb) one can notice that the long-range chemical ordering is reported only for $PbFe_{1/2}Sb_{1/2}O_3$ (PFS)[22,23] in contrast to $PbFe_{1/2}Nb_{1/2}O_3$ (PFN) and $PbFe_{1/2}Ta_{1/2}O_3$ (PFT) where random distribution of Fe^{3+} and Nb^{5+} (Ta^{5+}) ions in the lattice is observed.[24–27] Moreover, the experimental T_N values of both PFN and PFT (≈150 K)[4,5,8,23–27] are approximately in the middle between the theoretically predicted ones for completely disordered (≈300 K) and perfectly ordered (≈0 K) $PbFe_{1/2}B^{5+}{}_{1/2}O_3$ perovskites.[26,28] This contradiction is usually explained by the presence of partial local ordering (clustering) of Fe^{3+} and Nb^{5+} (Ta^{5+}) ions.[26,28] Studies of nuclear magnetic resonance (NMR),[29] Raman[30] and X-ray absorption spectra (XAFS),[31] measurements of acoustic emission[32] and magnetization,[33] as well as *ab initio* calculations[34] have shown that complex perovskites possess the very different macroscopic structure as compared with the local one. The dramatic (up to 100 K) increase in T_N values reported for PFN single-crystalline nanofilms[35] and mechanochemically synthesized PFN and PFT ceramics[36] was also ascribed to the changes in the degree of local ordering (clustering) of Fe^{3+} and Nb^{5+} (Ta^{5+}) ions.[34,36] It is worth mentioning that the effect of local ordering of Fe^{3+} and Nb^{5+} ions was also observed in the $BiFeO_3$–PFN solid solution system.[28] There is some evidence that even more sufficient changes in T_N due to compositional ordering can be achieved in the solid solution of $BiFeO_3$ with a highly ordered perovskite $PbFe_{1/2}Sb_{1/2}O_3$ (PFS).[37]

The scope of the present work was to study the compositional dependence of magnetic phase transition temperature T_N in two $BiFeO_3$-based solid solutions, containing as a second component highly ordered perovskites, namely $PbFe_{1/2}Sb_{1/2}O_3$ (PFS) and lead-free $SrFe_{1/2}Sb_{1/2}O_3$ (SFS). In order to exclude the effect of the Sr-substitution for Bi on T_N which is supposed to become noticeable at large enough (about 50% or more) degree of iron sublattice dilution[15] the content of SFS was limited to 60% which corresponds to 30% of Sb ions in the B-sublattice.

2. Experimental Methods

For synthesis of both $(1–x)BiFeO_3–xPbFe_{1/2}Sb_{1/2}O_3$ (BFO-*x*PFS) and $(1–x)BiFeO_3–xSrFe_{1/2}Sb_{1/2}O_3$ (BFO-*x*SFS) solid solution compositions, high pure Bi_2O_3, PbO, Fe_2O_3, $SrCO_3$ and preliminary synthesized $SbFeO_4$ were used as starting reagents. We mixed these reagents in a stoichiometric ratio, ground them in a ball mill in ethanol, dried them, and then fired at 870 °C in a closed alumina crucible for 20 min. The resulting product was ground in a ball mill and then fired at 1000 °C for 2 h.

We pressed synthesized powders into small disks of 4.5 mm in diameter and of ~4 mm in height. We carried out the synthesis under high pressure (4–6 GPa) in a DO-138A anvil press at 1300–1550 °C for 1–5 min, followed by quenching to room temperature. The atmosphere in the pressure vessel is slightly reducing[38]; therefore, the samples obtained in this way usually contain a fair amount of oxygen vacancies. These vacancies are intrinsic point defects in oxides of the perovskite family that arise most easily.[39] To reduce the concentration of oxygen vacancies as well as the residual mechanical stresses, the samples were annealed in air at 350–400 °C for 2 h prior to measurements.

$SrFe_{1/2}Sb_{1/2}O_3$ was prepared via solid phase reactions route using high-purity $SrCO_3$ and preliminary synthesized $SbFeO_4$. The components taken in stoichiometric proportions were well mixed in an agate mortar under ethanol. The synthesis was carried out in two stages: first, for 4 h at a temperature of 950 °C in a closed crucible made of aluminum oxide, then the reaction product was thoroughly ground by stirring in a mortar, then pressed into small disks, which were sintered for 2 h at 1300 °C.

X-ray diffraction (XRD) studies of the synthesized powders were performed at room temperature using DRON-3 diffractometer (CuKα radiation).

^{57}Fe Mössbauer spectra were measured with a MS1104Em spectrometer attached either to a helium cryostat CCS-850 or to a high-temperature furnace. The spectra were analyzed with the help of the SpectrRelax programm.[40] Isomer shifts were defined relative to the metallic α-Fe.

3. Results and Discussion

Room-temperature XRD studies revealed the formation of single-phase perovskite structure for all for the synthesized BFO – *x*SFS and BFO – *x*PFS samples. Figure 1 shows the XRD patterns for PFS and SFS samples. The reason that we

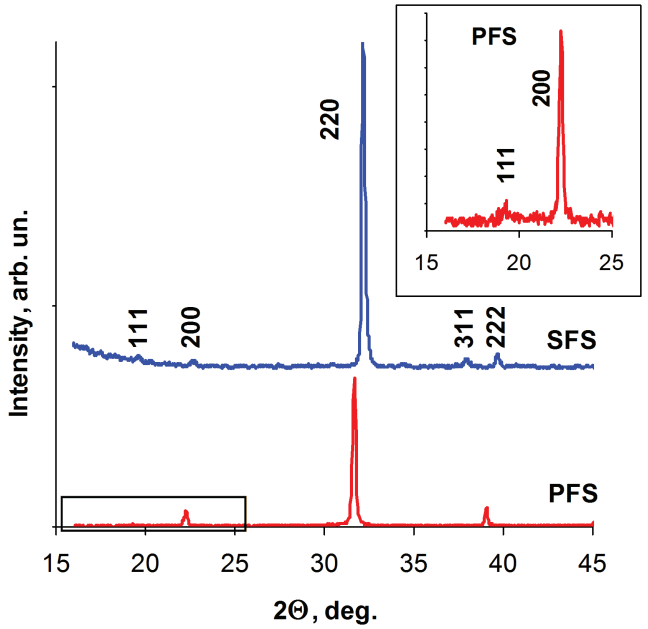

Fig. 1. Room-temperature XRD patterns of the PFS and SFS powders. The inset highlights the small-angle range for PFS where the superstructure (111) reflection is observed.

have shown these patterns in a relatively small angular range is to illustrate the formation of the perovskite phase. There is no parasitic pyrochlore phase and there are superstructural reflections that correspond to the doubling of the perovskite unit cell due to the ordering of Sb^{5+} and Fe^{3+} ions. We estimated the value of the degree of long-range compositional ordering S. Taking the ratio of the intensities of the fundamental and superstructural reflections,[16,17,29] we obtained an S value of 0.9 for PFS and 0.58 for SFS.

The XRD patterns of all the other BFO-*x*SFS and BFO-xPFS compositions studied show the well-formed perovskite structure and the lack of the superstructural reflections. As an example, Fig. 2 shows the XRD patterns for BFO-0.5SFS and BFO-0.5PFS samples.

In the compositional range of $x < 0.2$ for BFO-*x*SFS and $x < 0.35$ for BFO-*x*SFS, both solid solutions have a rhombohedral crystal structure (space group R3c) similar to that of $BiFeO_3$. At higher x values, XRD patterns for both systems generally correspond to the cubic perovskite structure, although the diffraction lines are somewhat broadened. This fact indicates that the crystal lattice of these perovskites is distorted and, strictly speaking, is not cubic. However, it is not possible to estimate the degree and type of such distortions, since the splitting of diffraction lines is not revealed using the available diffractometer. Interestingly, very similar changes of the structure with composition were reported recently for solid solution of $BiFeO_3$ with a disordered perovskite PFN.[41]

Figure 3 shows the compositional dependence of the lattice parameters for BFO-*x*SFS and BFO-*x*PFS solid solutions. For the sake of comparison, a similar dependence for BFO-*x*PFN

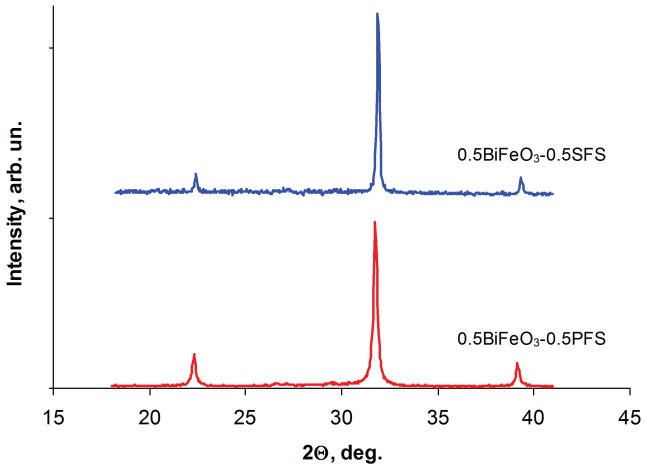

Fig. 2. Room-temperature XRD patterns of the $0.5BiFeO_3$-0.5PFS and $0.5BiFeO_3$-0.5SFS powders.

system is plotted using the data published in Ref. 41. Both the position and the width of the MPB between rhombohedral and pseudocubic phases are drawn very roughly just to mark their presence.

At room temperature, both PFS and SFS are in the paramagnetic phase and their Mössbauer spectra were successfully fitted with two components: a singlet and a doublet [Figs. 4(a) and 4(b)] in accord with the results of the previous studies of these compounds.[42,43] For all the other compositions studied room temperature, Mössbauer spectra were sextets indicating that they are in the magnetically ordered state. In order to have the possibility to compare the spectra of different solid solution compositions, the measurements

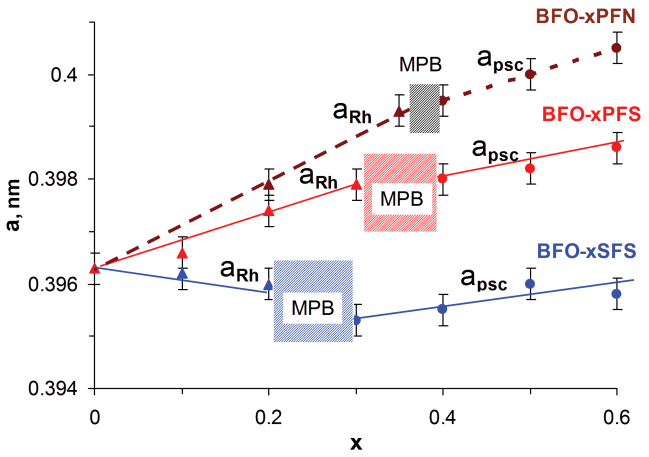

Fig. 3. Compositional dependences of the rhombohedral (a_{Rh}) and pseudocubic (a_{psc}) lattice parameters for BFO-*x*SFS and BFO-*x*PFS solid solutions. For comparison, a similar dependence for BFO-*x*PFN system is plotted using the data published in Ref. 41. Morphotropic phase boundaries (MPB) between rhombohedral and pseudocubic phases are drawn very roughly just to mark their presence.

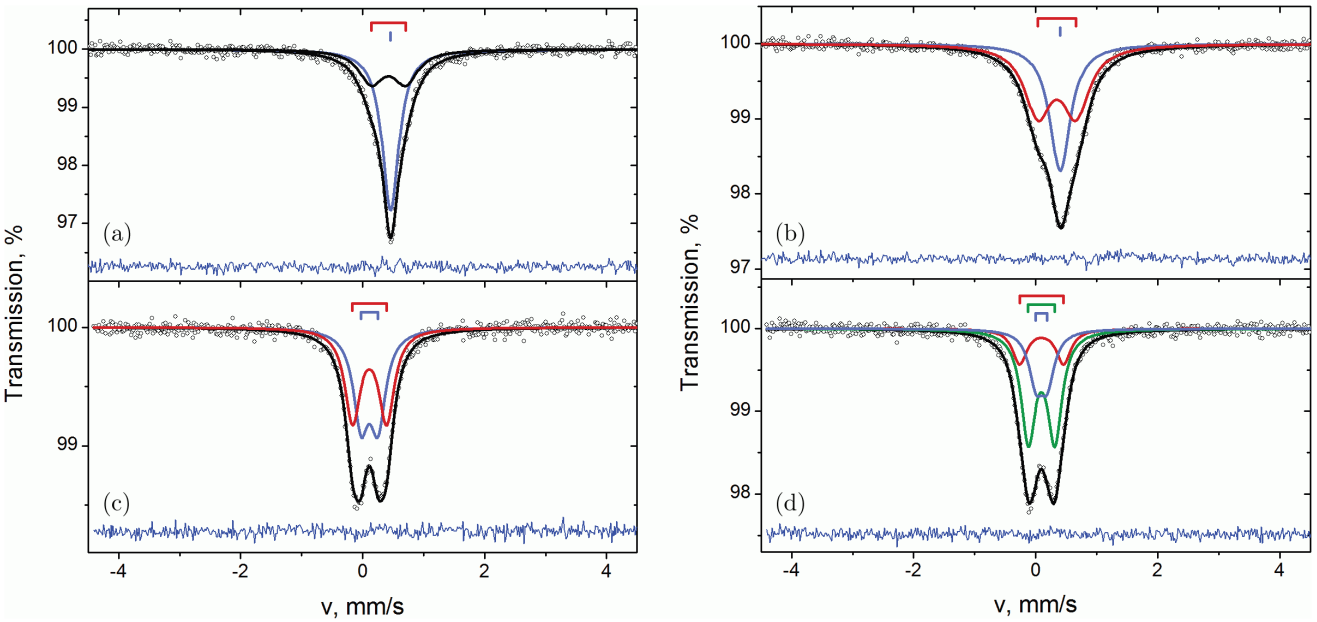

Fig. 4. Mössbauer spectra of (a) PFS, (b) SFS, (c) BFO-0.5PFS, (d) BFO-0.5SFS measured in the paramagnetic phase (at room temperature for PFS and SFS and at 723 K for BFO-0.5PFS and BFO-0.5SFS).

Table 1. Parameters of the Mössbauer spectra measured in the paramagnetic phase for the compositions studied.

Sample	T, K	Component	δ ± 0.02, mm/s	Δ ± 0.02, mm/s	Γ ± 0.02, mm/s	A ± 1, %	χ^2
PFS	295	S	0.46		0.33	63	1.140
		D1	0.44	0.56	0.48	37	
SFS	295	S	0.40		0.41	42	1.066
		D1	0.38	0.62	0.53	58	
$0.5BiFeO_3$–0.5PFS	723	D1	0.11	0.28	0.31	49	0.983
		D2	0.11	0.56	0.31	51	
$0.5BiFeO_3$–0.5SFS	723	D1	0.10	0.72	0.29	18	0.954
		D2	0.10	0.44	0.29	57	
		D3	0.10	0.19	0.29	25	

Notes: S: singlet, D: doublet, δ: isomer shift, Δ: quadrupole splitting for paramagnetic component, Γ: linewidth, A: component area, χ^2: Pearson criterion.

were carried out in the paramagnetic phase at 723 K. The results obtained for BFO-0.5PFS and BFO-0.5SFS compositions are displayed in Fig. 4 (panels c and d). The components' parameters of these spectra are shown in Table 1. For all the compositions studied, the values of isomer shift δ in the Mössbauer spectra correspond to Fe^{3+} in an octahedral environment taking account of the decrease of δ with temperature.[44,45]

As was already mentioned, the Mössbauer spectra of highly ordered PFS and SFS samples include both singlet and doublet components [Figs. 4(a) and 4(b)]. The singlet seems to correspond to the chemically ordered regions (quite large in size), while the doublet can be ascribed to the regions in which this long-range order is violated. Each Fe ion displaced from its sublattice affects the spectrum of several neighboring iron ions. That is why the fractions of singlet in the ^{57}Fe Mössbauer spectra for both PFS and SFS are substantially lower than the values of long-range ordering degree S of the same samples estimated using the XRD data.

Mössbauer spectrum of the BFO-0.5PFS sample [Fig. 4(c)] consists of two paramagnetic doublets, D1 and D2. The appearance of the quadrupole splitting is due to the presence of compositional disorder in the sample. Similar to macroscopically disordered perovskites, PFN and PFT this disorder may be ascribed to the clustering of Fe and Sb ions, i.e., that the sample contains regions where the concentration of Fe^{3+} ions is higher or lower than the average one.[33,34] The value of the quadrupole splitting Δ is related to the symmetry

of the local environment of Fe^{3+} ions. Since the D1 doublet has a smaller value of Δ, it matches the more symmetric surroundings of Fe^{3+} ions, which is more probable in zones where the concentration of these ions is high. The D2 doublet having a larger value of Δ seems to be due to the Fe^{3+} ions in the regions with a low Fe content.

Three doublets D1, D2, and D3 are present in the Mössbauer spectrum of the BFO-0.5SFS sample. Nearly, the same δ values of these doublets match to Fe^{3+} ions in an octahedral oxygen environment. The existence of above-mentioned doublets, corresponding to three types of local surroundings of the Fe^{3+} ions indicates that compositional inhomogeneity of BFO-0.5SFS is larger as compared to BFO-0.5PFS.

The temperature of magnetic phase transition (T_N) was retrieved using the intensity of the Mössbauer spectrum (I_m) measured in the velocity range 0–1.2 cm/s at different temperatures. In the vicinity of the magnetic phase transition, Mössbauer spectrum turns from a doublet or singlet to a sextet and the intensity of the spectrum within the above-mentioned velocity range decreases dramatically. Thus, the abrupt drop in the $I_m(T)$ curve corresponds to the T_N. Figure 5 shows the $I_m(T)$ dependences for the compositions studied. One can see that while the $I_m(T)$ dependences for PFS and SFS are very similar (see the inset in Fig. 5), the steps in the $I_m(T)$ curves corresponding to the BFO-xSFS samples are much more diffused as compared to the BFO-xPFS ones. Such difference is in line with the difference in the Mössbauer spectra of BFO-0.5SFS and BFO-0.5PFS compositions which was discussed above.

Figure 6 shows the $T_N(x)$ dependences for BFO-xPFS and BFO-xSFS solid solution systems, plotted using the data of Mössbauer studies. The dotted line shows the $T_N(x)$ dependence for BFO-xPFN system plotted using the results of the magnetization measurements.[28] The results of the subsequent magnetization, dielectric, and structural studies of several BFO-xPFN compositions are in a good agreement with this $T_N(x)$ curve.[46,47]

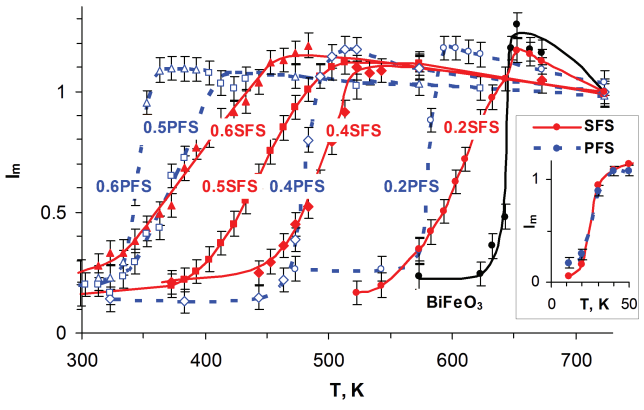

Fig. 5. Temperature dependences of the Mössbauer spectrum intensity I_m in the 0–1.2 mm/s range related to its value at the highest measuring temperature for BFO-xSFS (solid lines) and BFO-xPFS (broken lines) compositions. The inset shows the $I_m(T)$ dependences for SFS and PFS.

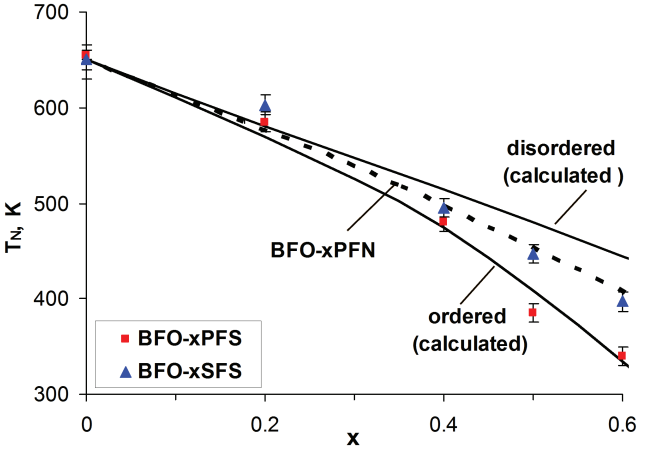

Fig. 6. Concentration dependences of the magnetic phase transition temperature T_N for BFO-xSrFS and BFO-xPFS solid solutions plotted using the data of Mössbauer studies. Black solid lines show the $T_N(x)$ dependences for $(1-x)BiFeO_3$–$xPbFe_{1/2}B^{5+}{}_{1/2}O_3$ solid solutions calculated for the cases of the ordered and disordered distribution of Fe^{3+} and non-magnetic B^{5+} ions in the lattice[28]. The broken line between two calculated ones shows the experimental $T_N(x)$ dependence for BFO-xPFN ceramics plotted using the results of the magnetization measurements.[28]

One can see that the $T_N(x)$ dependence for BFO-xPFN system lies approximately halfway between the $T_N(x)$ dependences for $(1-x)BiFeO_3$–$xPbFe_{1/2}B^{5+}{}_{1/2}O_3$ solid solutions calculated for the cases of the ordered and disordered distribution of Fe^{3+} and nonmagnetic B^{5+} ions in the lattice.[28] This result is usually interpreted as an evidence of the short-range ordering of Fe^{3+} and Nb^{5+} ions in PFN. Unlike this, the $T_N(x)$ dependence for solid solution of BFO with a highly ordered perovskite PFS appears to be very close to the one calculated for the $(1-x)BiFeO_3$–$xPbFe_{1/2}B^{5+}{}_{1/2}O_3$ solid solutions under the assumption of the complete ordering of Fe^{3+} and nonmagnetic B^{5+} ions in the lattice.[28] It is rather surprising as no evidence of the long-range ordering of Fe^{3+} and Sb^{5+} ions were observed in the XRD patterns and in Mössbauer spectra of the BFO-xPFS compositions studied. Even more surprising is the fact that T_N values of the BFO-xSrFS compositions studied match $T_N(x)$ curve for the BFO-xPFN rather than that for BFO-xPFS, though SrFS is also a highly ordered perovskite like PFS. One of the possible origins of this discrepancy may be the difference in the lattice parameters of BFO-xPFS and BFO-xSFS compositions. As one can see in Fig. 3, lattice parameters for both the rhombohedral (a_{Rh}) and pseudocubic (a_{psc}) compositions of BFO-xPFS are larger than those of the similar BFO-xSFS ones and this difference increases as x grows. It is widely known that the increase of the distance between magnetic ions caused by the increase of the lattice parameter usually leads to a dramatic decrease of the magnetic exchange and corresponding lowering of T_N.[48,49] However the difference in the T_N values of BFO-xPFS and BFO-xSFS compositions becomes visible only in the $x > 0.4$

range while the difference in the lattice parameters becomes substantial at lower x values. Moreover, for BFO-PFN system both the a_{Rh} and a_{psc} values are even larger than those for similar BFO-xPFS ones (Fig. 3) while the T_N values are higher, especially in the $x > 0.4$ range. Thus it seems that the difference in T_N values between BFO-xPFS and BFO-xSFS compositions is due to the difference in the chemical (compositional) ordering degree of Fe^{3+} and Sb^{5+} ions. This ordering may be short-range and local and thus not detectable by the XRD.

4. Summary

Ceramic samples of $BiFeO_3$-based perovskite solid solutions with the highly-ordered complex perovskites $PbFe_{1/2}Sb_{1/2}O_3$ (PFS) and $SrFe_{1/2}Sb_{1/2}O_3$ (SFS) were obtained using high-pressure synthesis at 4–6 GPa. Compositional range of both $(1–x)BiFeO_3–xPbFe_{1/2}Sb_{1/2}O_3$ (BFO-PFS) and $(1–x)BiFeO_3–xSrFe_{1/2}Sb_{1/2}O_3$ (BFO-SFS) solid solutions was limited to $0 \le x \le 0.6$ to exclude the possible effect of excess diluting of both Bi- and Fe- sublattices on the magnetic phase transition temperature T_N. Neither XRD nor Mössbauer studies detected the presence of the long-range chemical ordering in the compositions studied except PFS and SFS. Mössbauer studies revealed that $BiFeO_3$-SFS compositions are characterized by a larger compositional inhomogeneity as compared to $BiFeO_3$-PFS ones. In line with this result concentration dependence of the magnetic phase transition temperature T_N for $BiFeO_3$-SFS compositions was found to be close to the $T_N(x)$ dependence for $BiFeO_3$ solid solution with disordered perovskite $PbFe_{1/2}Nb_{1/2}O_3$ (PFN). In contrast to this T_N(x) dependence for $BiFeO_3$-PFS compositions nicely follows the theoretical $T_N(x)$ dependence calculated for the case of the ordered distribution of Fe^{3+} and non-magnetic Sb^{5+} ions in the lattice. The difference in T_N values between BFO-xPFS and BFO-xSFS compositions seems to be due to the difference in the chemical (compositional) ordering degree of Fe^{3+} and Sb^{5+}. This ordering is likely to be short-range and local and thus not detectable by the XRD.

Acknowledgments

The reported study was funded by RFBR (Project number 20-52-00045) and BRFBR (Project number T20R-169).

References

[1]G. Catalan and J. F. Scott, Physics and applications of bismuth ferrite, *Adv. Mater.* **21**, 2463 (2009).

[2]D. I. Khomskii, Multiferroics: Different ways to combine magnetism and ferroelectricity, *J. Magn. Magn. Mater*. **306**(1), 1 (2006).

[3]W. Eerenstein, N. D. Mathur and J. F. Scott, Multiferroic and magnetoelectric materials, *Nature* **442**, 759 (2006).

[4]D. A. Sanchez, N. Ortega, A. Kumar, G. Sreenivasulu, R. S. Katiyar, J. F. Scott, D.M. Evans, M. Arredondo-Arechavala, A. Schilling and J. M. Gregg, Room-temperature single phase multiferroic magnetoelectrics: $Pb(Fe,M)_x(Zr,Ti)_{(1–x)}O_3$ [M=Ta, Nb], *J. Appl. Phys*. **113**, 074105 (2013).

[5]V. V. Laguta, A. N. Morozovska, E. I. Eliseev, I. P. Raevski, S. I. Raevskaya, E. I. Sitalo, S. A. Prosandeev and L. Bellaiche, Room-temperature paramagnetoelectric effect in magnetoelectric multiferroics $Pb(Fe_{1/2}Nb_{1/2})O_3$ and its solid solution with $PbTiO_3$, *J. Mater. Sci*. **51**, 5330 (2016).

[6]M. Azuma, H. Kanda, A. A. Belik, Y. Shimakawa and M. J. Takano, Magnetic and structural properties of $BiFe_{1–x}Mn_xO_3$, *J. Magn. Magn. Mater*. **310**, 1177 (2007).

[7]M. D. Glinchuk, E. A. Eliseev and A. N. Morozovska, Novel room temperature multiferroics on the base of single-phase nanostructured perovskites, *J. Appl. Phys*. **116**, 054101 (2014).

[8]V. V. Laguta, V. A. Stephanovich, I. P. Raevski, S. I. Raevskaya, V. V. Titov, V. G. Smotrakov and V. V. Eremkin, Magnetoelectric effect in antiferromagnetic multiferroic $Pb(Fe_{1/2}Nb_{1/2})O_3$ and its solid solutions with $PbTiO_3$, *Phys. Rev. B* **95**, 014207 (2017).

[9]B. Fraygola, A. A. Coelho and J. A. Eiras, Magnetoelectric coupling in $Pb(Fe,W)O_3$ based ceramics, *Ferroelectrics*, **442**(1), 50 (2013).

[10]D. D. Khalyavin, A. N. Salak, N. M. Olekhnovich, A. V. Pushkarev, Y. V. Radyush, P. Manuel, I. P. Raevski, M. L. Zheludkevich and M. G. S. Ferreira, Polar and antipolar polymorphs of metastable perovskite $BiFe_{0.5}Sc_{0.5}O_3$, *Phys. Rev. B* **89**, 174414 (2014).

[11]M. A. Gilleo, Superexchange interaction in ferromagnetic garnets and spinels which contain randomly incomplete linkages, *J. Phys. Chem. Sol*. **13**(1–2), 33 (1960).

[12]I. P. Raevski, S. P. Kubrin, S. I. Raevskaya, S. A. Prosandeev, D. A. Sarychev, M. A. Malitskaya, V. V. Stashenko and I. N. Zakharchenko, Studies of ferroelectric and magnetic phase transitions in $Pb_{1–x}A_xFe_{1/2}Nb_{1/2}O_3$ (A–Ca, Ba) solid solutions, *Ferroelectrics* **398**(1), 16 (2010).

[13]K. Kimura, K. Yokochi, R. Kondo, D. Urushihara, Y. Yamamoto, A. K. R. Ang, N. Happo, K. Ohara, T. Matsushita, T. Asaka, M. Iwata and K. Hayashi, Local structural analysis of $Pb(Fe_{1/2}Nb_{1/2})O_3$ multiferroic material using X-ray fluorescence holography, *Jpn. J. Appl. Phys.* **58**, 100601 (2019).

[14]R. de Sousa, M. Allen and M. Cazayous, Theory of spin-orbit enhanced electric-field control of magnetism in multiferroic $BiFeO_3$, *Phys. Rev. Lett*. **110**, 267202 (2013).

[15]S. I. Raevskaya, S. P. Kubrin, J. Zhuang, I. P. Raevski, M. A. Malitskaya, I. N. Zakharchenko, M. S. Panchelyuga and V. V. Titov, Mössbauer and magnetization studies of magnetic phase transitions in $0.5BiFeO_3–0.5NaNbO_3$ and $0.5LaFeO_3–0.5NaNbO_3$ solid solutions, *J. Adv. Dielectr*. **10**(1–2), 2060005 (2020).

[16]N. Setter and L. E. Cross, The role of B-site cation disorder in diffuse phase transition behavior of perovskite ferroelectrics. *J. Appl. Phys*. **51**(8), 4356 (1980).

[17]I. P. Raevski, S. A. Prosandeev, S. M. Emelyanov, F. I. Savenko, I. N. Zakharchenko, O. A. Bunina, A. S. Bogatin, S. I. Raevskaya, E. S. Gagarina, E. V. Sahkar and L. Jastrabik, Random-site cation ordering and dielectric properties of $PbMg_{1/3}Nb_{2/3}O_3–PbSc_{1/2}Nb_{1/2}O_3$. // *Integr. Ferroelectrics* **53**, 475 (2003).

[18]A. A. Bokov, I. P. Raevski and V. G. Smotrakov, Composition, ferroelectric, and antiferroelectric ordering in Pb_2InNbO_6 crystals, *Fizika Tverd. Tela* **26**(8), 2824 (1984). (*Sov. Phys. Solid State*. **26**(9), 1708 (1984)).

[19]K. Ohwada and Y. Tomita, Experiment and theory of $Pb(In_{1/2}Nb_{1/2})O_3$: Antiferroelectric, ferroelectric, or relaxor state depending on perovskite B-site randomness, *J. Phys. Soc. Jpn*. **79**, 011012 (2010).

[20]C. Cochard, X. Bril, O. Guedes and P. E. Janolin, Interpretation of polar orders based on electric characterizations: Example of $Pb(YbNb)O_3–PbTiO_3$ solid solution, *J. Electron. Mater*. **45**(11), 6005 (2016).

[21]P. K. Davies, H. Wu, A. Y. Borisevich, I. E. Molodetsky and L. Farber, Crystal chemistry of complex perovskites: New cation-ordered dielectric oxides, *Annu. Rev. Mater Res*. **38**, 369 (2008).
[22]V. V. Laguta, V. A. Stephanovich, M. Savinov, M. Marysko, R. O. Kuzian, N. M. Olekhnovich, A. V. Pushkarev, Yu.V. Radyush, I. P. Raevski, S. I. Raevskaya and S. A. Prosandeev, Superspin glass phase and hierarchy of interactions in multiferroic $PbFe_{1/2}Sb_{1/2}O_3$: An analog of ferroelectric relaxors? *New J. Phys*. **16**, 11304 (2014).
[23]B. Argymbek, T. Kmjec, V. Chlan, J. Kohout, S. E. Kichanov, D. P. Kozlenko and B. N. Savenko, The crystal and magnetic structures of the ordered perovskite Pb_2FeSbO_6 studied by neutron diffraction and Mössbauer spectroscopy, *J. Magn. Magn. Mater*. **477**, 334 (2019).
[24]N. Lampis, P. Sciau and A. Geddo Lehmann, Rietveld refinements of the paraelectric and ferroelectric structures of $PbFe_{0.5}Nb_{0.5}O_3$, *J. Phys.: Condens. Matter* **11**, 3489 (1999).
[25]S. A. Ivanov, R. Tellgren, H. Rundlof, N. W. Thomas and S. Ananta, Investigation of the structure of the relaxor ferroelectric $Pb(Fe_{1/2}Nb_{1/2})O_3$ by neutron powder diffraction, *J. Phys.: Condens. Matter* **12**, 2393 (2000).
[26]S. Nomura, H. Takabayashi and T. Nakagawa, Dielectric and magnetic properties of $Pb(Fe_{1/2}Ta_{1/2})O_3$, *Jpn. J. Appl. Phys*. **7**, 600 (1968).
[27]A. Kania, S. Miga, E. Talik, I. Gruszka, M. Szubka, M. Savinov, J. Prokleska and S. Kamba, Dielectric and magnetic properties, and electronic structure of multiferroic perovskite $PbFe_{0.5}Ta_{0.5}O_3$ and incipient ferroelectric pyrochlore $Pb_2Fe_{0.34}Ta_{1.84}O_{7.11}$ single crystals and ceramics, *J. Eur. Ceram. Soc*. **36**, 3369 (2016).
[28]G. A. Smolenskii and V. M. Yudin, Weak ferromagnetism of some bismuth oxide-lead oxide-iron oxide-niobium oxide perovskites, *Sov. Phys.-Solid St*. **6**, 2936 (1965).
[29]Yu. O. Zagorodniy, R. O. Kuzian, I. V. Kondakova, M. Marysko, V. Chlan, H. Štěpánková, N. M. Olekhnovich, A. V. Pushkarev, Yu.V. Radyush, I. P. Raevski, B. Zalar, V. V. Laguta and V. A. Stephanovich, Chemical disorder and ^{207}Pb hyperfine fields in the magnetoelectric multiferroic $Pb(Fe_{1/2}Sb_{1/2})O_3$ and its solid solution with $Pb(Fe_{1/2}Nb_{1/2})O_3$, *Phys. Rev. Mater.* **2**, 014401 (2018).
[30]N. S. Druzhinina, Yu. I. Yuzyuk, I. P. Raevski, M. El Marssi, V. V. Laguta and S. I. Raevskaya, Raman spectra of $PbFe_{0.5}Nb_{0.5}O_3$ multiferroic single crystals and ceramics, *Ferroelectrics* **438**(1), 107 (2012).
[31]V. A. Shuvaeva, I. Pirog, Y. Azuma, K. Yagi, K. Sakaue, H. Terauchi, I. P. Raevskii, K. Zhuchkov and M. Yu, Antipin, The local structure of mixed-ion perovskites, *J Phys: Condens Matter* **15**, 2413 (2003).
[32]E. Dul'kin, E. Mojaev, M. Roth, I. P. Raevski and S. A. Prosandeev, Nature of thermally stimulated acoustic emission from $PbMg_{1/3}Nb_{2/3}O_3$–$PbTiO_3$ solid solutions, *Appl. Phys. Lett*. **94**, 252904 (2009).
[33]W. Kleemann, V. V. Shvartsman, P. Borisov and A. Kania, Coexistence of antiferromagnetic and spin cluster glass order in the magnetoelectric relaxor multiferroic $PbFe_{0.5}Nb_{0.5}O_3$, *Phys. Rev. Lett*. **105**, 257202 (2010).
[34]S. A. Prosandeev, I. P. Raevski, S. I. Raevskaya and H. Chen, Influence of epitaxial strain on clustering of iron in $Pb(Fe_{1/2}Nb_{1/2})O_3$ thin films, *Phys. Rev. B* **92**, 220419(R) (2015).
[35]W. Peng, N. Lemee, M. Karkut, B. Dkhil, V. Shvartsman, P. Borisov, W. Kleemann, J. Holc, M. Kosec and R. Blinc, Spin-lattice coupling in multiferroic $Pb(Fe_{1/2}Nb_{1/2})O_3$ thin films, *Appl. Phys. Lett*. **94**, 012509 (2009).
[36]A. A. Gusev, S. I. Raevskaya, V. V. Titov, E. G. Avvakumov, V. P. Isupov, I. P. Raevski, H. Chen, C.-C. Chou, S. P. Kubrin, S. V. Titov, M. A. Malitskaya, A. V. Blazhevich, D. A. Sarychev, V. V. Stashenko and S. I. Shevtsova, Dielectric and Mossbauer studies of $Pb(Fe_{1/2}Ta_{1/2})O_3$ multiferroic ceramics sintered from mechanoactivated powders, *Ferroelectrics* **475**(1), 41 (2015).
[37]I. P. Raevski, S. P. Kubrin, A. V. Pushkarev, N. M. Olekhnovich, Y. V. Radyush, G. R. Li, C.-C. Chou, S. I. Raevskaya, V. V. Titov and M. A. Malitskaya, Magnetic phase transitions in solid solutions of Fe-containing perovskite multiferroics, *Ferroelectrics*, **542**(1), 36 (2019).
[38]V. A. Stephanovich, V. Laguta, M. Marysko, I. Raevsky, N. Olekhnovich, A. Pushkarev, Y. Radyush, S. Raevskaya, R. Kuzian, V. Chlan and H. Štěpánková, Cluster superconductivity in the magnetoelectric $Pb(Fe_{1/2}Sb_{1/2})O_3$ ceramics, *Acta Phys. Pol. A* **131**(6), 1534 (2017).
[39]S. A. Prosandeev, A. V. Fisenko, A. V. Riabchinski, I. A. Osipenko, I. P. Raevski and N. Safontseva, Study of intrinsic point defects in oxides of the perovskite family, I Theory, *J. Phys.: Condens. Matter* **8**, 6705 (1996).
[40]M. E. Matsnev and V. S. Rusakov, SpectrRelax: An application for Mössbauer spectra modeling and fitting, *AIP Conf. Proc*. **1489** 178 (2012).
[41]L. A. Shilkina, A. V. Pavlenko, L. A. Reznitchenko and I. A. Verbenko, Phase diagram of the system of $(1–x)BiFeO_3$–$xPbFe_{0.5}Nb_{0.5}O_3$ solid solutions at room temperature, *Crystallogr. Rep*. **61**(2), 263 (2016).
[42]P. D. Battle, T. C. Gibb, A. J. Herod and J P. Hodges, Sol-gel synthesis of the magnetically frustrated oxides Sr_2FeSbO_6 and $SrLaFeSnO_6$, *J. Mater. Chem*. **5**(l), 75 (1995).
[43]I. P. Raevski, N. M. Olekhnovich, A. V. Pushkarev, Y. V. Radyush, S. P. Kubrin, S. I. Raevskaya, M. A. Malitskaya, V. V. Titov and V. V. Stashenko, Mössbauer studies of $PbFe_{0.5}Nb_{0.5}O_3$–$PbFe_{0.5}Sb_{0.5}O_3$ multiferroic solid solutions, *Ferroelectrics* **444**(1), 47 (2013).
[44]F. Menil, Systematic trends of the ^{57}Fe Mössbauer isomer shifts in (FeO_n) and (FeF_n) polyhedra. Evidence of a new correlation between the isomer shift and the inductive effect of the competing bond T-X (*Fe) (Where X is O or F and T is any element with a formal positive charge), *J. Phys. Chem. Solids* **46**(7), 763 (1985).
[45]V. N. Lebedev, Temperature dependence of the isomeric Mössbauer -spectrum shift of weakly covalent compounds of the Fe^{3+} ion, *Sov. Phys. J.* **21**, 41 (1978).
[46]J. P. Patel, A. Senyshyn, H. Fuess and D. Pandey, Evidence for weak ferromagnetism, isostructural phase transition, and linear magnetoelectric coupling in the multiferroic $Bi_{0.8}Pb_{0.2}Fe_{0.9}Nb_{0.1}O_3$ solid solution, *Phys. Rev. B* **88**, 104108 (2013).
[47]U. Prah, M. Wencka, T. Rojac, A. Benčana and H. Uršič, $Pb(Fe_{0.5}Nb_{0.5})O_3$–$BiFeO_3$–based multicalorics with room-temperature ferroic anomalies, *J. Mater. Chem. C* **8**, 11282 (2020).
[48]J. B. Goodenough, *Magnetism and Chemical Bond* (Interscience Publisher, 1963).
[49]M. Eibschutz, S. Shtrikman and D. Treves, Mössbauer studies of Fe^{57} in orthoferrites, *Phys. Rev*. **156**(2), 562 (1967).